

# Dependence of damage efficiency of ions in diamond on electronic stopping

E. Friedland <sup>a,\*</sup>, H.D. Carstanjen <sup>b</sup>, G. Myburg <sup>a</sup>, M.A. Nasr <sup>a,c</sup>

<sup>a</sup> Department of Physics, University of Pretoria, 0002 Pretoria, South Africa

<sup>b</sup> Max-Planck-Institut für Metallforschung, Heisenbergstr. 1, D-70569 Stuttgart, Germany

<sup>c</sup> Department of Physics, Misurata University, Libya

Available online 22 January 2005

## Abstract

Natural diamond single crystals were irradiated at room temperature with 75 keV carbon and 80 keV argon ions at fluences exceeding the graphitization dose. The resulting damage depth profiles before and after rapid annealing at 1500 K were obtained by  $\alpha$ -particle channeling analysis. Measurements were done both at back- and forward scattering angles using conventional surface barrier detectors and an electrostatic analyzer system, respectively. Boundary positions of the graphitic layers were determined and compared with the corresponding depth-dependent elastic and inelastic energy deposition graphs to extract critical damage energy densities. The obtained values increase strongly with inelastic energy deposition rate, indicating a significant reduction of the ions' damage efficiency due to irradiation induced annealing by electronic stopping.

© 2004 Elsevier B.V. All rights reserved.

**Keywords:** Diamond; Ion implantation; Phase transition

## 1. Introduction

Of the many allotropic forms of carbon, diamond is one of the most intriguing and unique materials. It is the hardest material known with the highest atomic density of any solid, possessing also the highest thermal conductivity, although

being essentially an insulator. These and other exceptional physical properties have attracted much attention in recent years both from fundamental science and technology.

At ambient conditions the thermodynamical stable form of solid carbon is graphite and diamond is therefore in principle unstable, transforming very slowly from its  $sp^3$  state to the graphitic  $sp^2$  state. From thermal graphitization studies [1] the energy barrier separating these two phases can be estimated to be of the order of a few eV. Exposure to energetic particle bombardment

\* Corresponding author. Tel.: +27 12 420 2453; fax: +27 12 362 5288.

E-mail address: [fried@scientia.up.ac.za](mailto:fried@scientia.up.ac.za) (E. Friedland).

should therefore lead to the rapid transformation of diamond to the lower energy state of graphite. In spite of this expectation, numerous implantation studies have demonstrated a remarkable radiation hardness of diamond. At room temperature irreversible phase transition to the graphitic state is only observed at fluences transferring damage energy densities above 10 eV/atom to the diamond lattice at the elastic stopping power maximum [2–4].

However, a detailed analysis of graphitization profiles after carbon implantation shows a dramatic decrease of the minimum damage energy density necessary for graphitization near the ions' end of range, where electronic stopping becomes negligible [5]. This behaviour of the critical damage energy density, in the following referred to as graphitization energy, seems to indicate strong annealing effects due to inelastic energy deposition, which significantly reduces the damage efficiency of the elastic collision processes at smaller depths. To further investigate this suspected dependence, graphitization energies must be determined for heavier ions, where the inelastic energy deposition rate becomes more important. In this work damage profiles for carbon and argon implantations at fluences exceeding amorphization doses are compared.

## 2. Experimental method and data analysis

Natural diamond samples of type IIa were cut perpendicular to the  $\langle 111 \rangle$  or  $\langle 100 \rangle$  directions, mechanically polished and subsequently annealed for 10 min at 1700 K in an argon atmosphere before being implanted at room temperature with either 75 keV carbon or 80 keV argon ions. To reduce channeling as far as possible, targets were tilted by  $7^\circ$  relative to the surface normal. Dose rates were kept below  $10^{13} \text{ cm}^{-2} \text{ s}^{-1}$  to prevent non-linear effects during collision cascade evolution. Fluences of either  $6 \times 10^{15} \text{ cm}^{-2} \text{ C}^+$  or  $1.5 \times 10^{15} \text{ cm}^{-2} \text{ Ar}^+$  were used to create severely damaged layers in the surface region. After implantation the targets were subjected to a rapid heating cycle of 15 min each at a temperature of approximately 1500 K under a protective argon

atmosphere. The reason for this high-temperature annealing will be discussed in Section 3.

After each step  $\alpha$ -particle channeling spectra were recorded, employing two different experimental techniques. For fast analyses of damage profiles, a conventional system using a silicon detector at a backscattering angle of  $165^\circ$  is used in conjunction with a three-axis goniometer. In this case channeling is observed along the crystallographic axis near the surface normal and energy calibration is obtained by comparing spectra for beam energies of 1.5 and 1.8 MeV. The analyzing particle beam was collimated to obtain a beam spot of 1 mm diameter on the target with a divergence of less than  $0.04^\circ$ . Beam current was approximately 15 nA and was measured directly on the target. To suppress secondary electrons a ring-shaped electrode in front of the target was kept at a negative potential of 300 V. The channeling spectra were normalized to random spectra collected during rotation of the sample about an axis tilted by approximately  $5^\circ$  relative to the channeling direction. The energies of the backscattered  $\alpha$ -particles are converted to a depth scale by using the energy loss data of Ziegler [6]. Depth resolution near the surface is limited by the detector's energy resolution of 12 keV to approximately 15 nm.

To obtain higher depth resolution some channeling spectra were also taken at a forward scattering angle of  $75^\circ$ , employing an electrostatic analyzer system combined with a position-sensitive detector [7]. For these measurements samples had to be tilted to align the  $\alpha$ -particle beam with the  $\langle 110 \rangle$  orientation. A similar beam spot size as in the previous set-up was used at a current of approximately 60 nA, which was measured by a beam chopper. Relative energy resolution of this spectrometer is of the order of 0.002 for the position-sensitive silicon detector used in this experiment and depth resolution is therefore only limited by energy straggling within the target. However, the small energy window of 2.8% together with an acceptance solid angle of  $\Delta\Omega \sim 0.15 \text{ msr}$  made measurements rather time-consuming. As up to 30 different spectrometer settings had to be used to cover depths exceeding 100 nm, only aligned spectra were measured, which were then normalized to the random spectra

from the backscattering analysis. In most of the measurements  $\text{He}^{2+}$  ions were observed, although some spectra for  $\text{He}^+$  ions were also taken. The collected data were corrected for the energy dependence of the charge state distribution using the tables of Marion and Young [8]. Energy calibration was obtained directly from the spectrometer setting. All spectra were taken using the same incident beam energy of 1 MeV and then corrected for the linear dependence of the channel width on energy.

### 3. Experimental results

Regarding the analysis of the aligned spectra, it has to be stressed that reaching the random level does not necessarily mean graphitization. During damage accumulation the increasing collisional disorder seems to change only gradually from the original  $\text{sp}^3$  to  $\text{sp}^2$  or even  $\text{sp}^1$  bonding. Even in a totally disordered layer the  $\text{sp}^3$  state may still be the dominant phase, allowing restructuring of the diamond lattice during high-temperature annealing. Only after reaching a critical concentration of  $\text{sp}^2$  bonds, annealing will lead to the collapse of the remaining diamond structure into the graphitic state. This hypothetical process of transforming crystalline diamond during ion bombardment at first predominantly into disordered diamond, which after further irradiation changes gradually into disordered graphite, is strongly supported by depth-resolved Raman spectroscopy [9] and atomic force microscopy combined with channeling analysis [2]. High-temperature annealing after implantation is therefore an essential step for determining graphitization energies.

An important parameter determining the concentration of destroyed  $\text{sp}^3$  bonds will be the damage energy density, defined as the average accumulated elastic energy transferred to a lattice atom during irradiation. To calculate this quantity one has to take into account that besides the primary ion also a recoiling atom loses an appreciable amount of its kinetic energy by inelastic collisions, so that only part of it is available for secondary elastic collisions. The total elastic energy transfer to an atom depends only weakly on binding and

displacement energies and is related to the nuclear stopping power. Due to its strong velocity dependence the energy transfer changes continuously along the ion's path and in addition will also be slightly influenced at larger depths by the diminishing irradiation dose due to range straggling. The total elastic energy density  $\tau_n(x)$  transferred to the lattice by a single ion at depth  $x$  can be calculated from TRIM-simulations [10] by combining the two elastic contributions of phonon excitation and atomic displacement and then subtracting the inelastic energy losses of the primary and secondary recoils [2]. The damage energy density accumulated during an implantation at a particular depth is then given by

$$\epsilon(x) = \tau_n(x)F/\rho,$$

where  $F$  is the fluence and  $\rho$  the atomic target density.

Fig. 1 shows an aligned spectrum acquired with the electrostatic analyzer spectrometer after implantation of 75 keV carbon ions into diamond and subsequent rapid annealing at 1500 K. Channeling spectra of the same sample taken for the

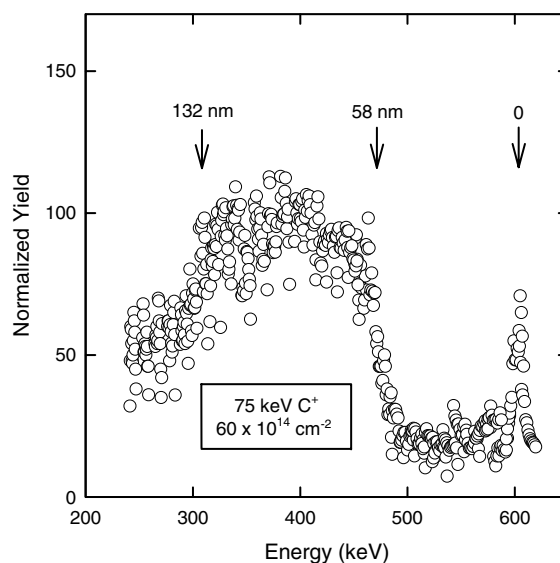


Fig. 1. Scattering spectrum of 1 MeV  $\alpha$ -particles aligned along the  $\langle 110 \rangle$  direction in diamond after 75 keV carbon implantation with a fluence of  $6 \times 10^{15} \text{ cm}^{-2}$ . The data were obtained with an electrostatic analyzer at a scattering angle of  $75^\circ$  and a target tilt angle of approximately  $40^\circ$ .

backscattering geometry show that the aligned spectrum reaches the random count rate at a region with the centre at about 100 nm. The energy of particles scattered from this depth is approximately 390 keV, which corresponds to the midpoint of the broad damage peak observed in Fig. 1. By normalizing the data at this energy, the boundaries of the buried graphitic layer are found to occur at depths of 58 nm and 132 nm.

An aligned spectrum after implantation of 80 keV argon ions, obtained in a similar way as discussed above, is displayed in Fig. 2, while the corresponding spectra for the backscattering geometry are shown in Fig. 3. Spectra A1 and A2 are taken before and after the final annealing at about 1500 K and reveal a slight increase of dechanneling beyond the damage peak after the thermal treatment due to removal of the remaining  $sp^3$  bonds. The inset in Fig. 3 shows a Raman spectrum from the surface region after annealing. It exhibits the shape expected for amorphous graphite with no trace of the narrow diamond line at  $1332\text{ cm}^{-1}$ . The graphitic layer seems to extend right from the surface up to a depth of 56 nm.

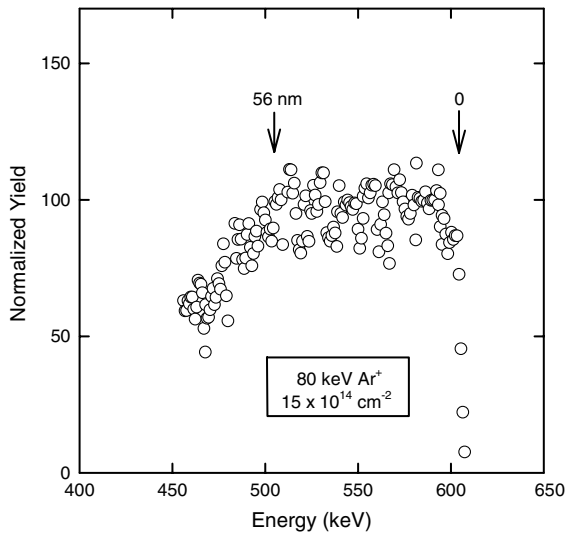


Fig. 2. Scattering spectrum of 1 MeV  $\alpha$ -particles aligned along the  $\langle 110 \rangle$  direction in diamond after 80 keV argon implantation with a fluence of  $1.5 \times 10^{15}\text{ cm}^{-2}$ . The data were obtained with an electrostatic analyzer at a scattering angle of  $75^\circ$  and a target tilt angle of approximately  $55^\circ$ .

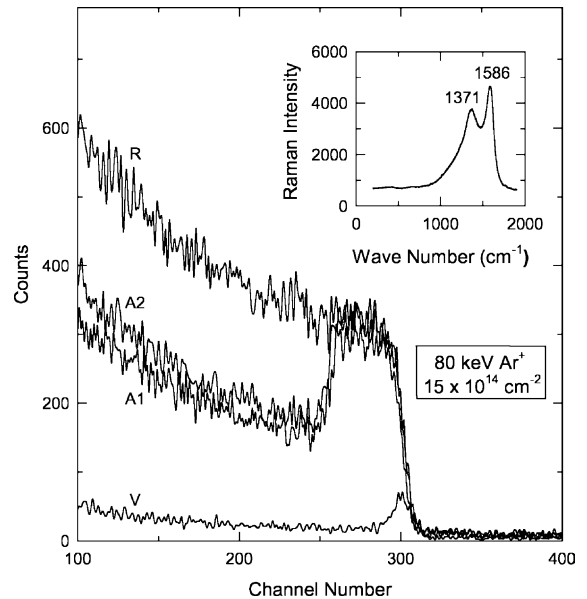


Fig. 3. Random (R) and aligned backscattering spectra for the  $\langle 100 \rangle$  direction before (A1) and after (A2) annealing at 1500 K for diamond implanted with an argon fluence exceeding the amorphization dose. Data were obtained with a surface barrier detector at a scattering angle of  $165^\circ$ . Also shown is the aligned spectrum before implantation (V). The inset shows the Raman spectrum after annealing.

In this context one should also consider the results of [11] for a 200 keV argon implant with a fluence of  $7 \times 10^{14}\text{ cm}^{-2}$ . Significant disorder was created by this implantation in the surface layer, leading to a damage peak in the aligned spectrum, which almost reaches the random level. However, channeling analysis revealed that the original diamond structure was reconstructed to a large extent after annealing at 1500 K. This was also confirmed by Raman spectroscopy, showing the typical sharp diamond line without any indication of a graphitic background after thermal annealing. The applied dose was obviously insufficient to exceed anywhere along the ions' range the critical  $sp^2$  concentration necessary for graphitization.

#### 4. Discussion and conclusions

To determine the critical damage energy densities for graphitization, elastic energy deposition

densities  $\tau_n$  were calculated as discussed above, assuming a displacement energy of 45 eV [12,13] and a binding energy of 5 eV. In a similar way inelastic energy deposition densities  $\tau_e$  were determined by adding the electronic energy losses of the recoils to that of the primary ion. The depth profiles of these two quantities for 75 keV carbon and 80 keV argon ions in diamond are displayed in the two graphs of Fig. 4. The experimentally obtained boundaries of the graphitized regions are indicated by arrows. However, it should be noted that for a direct comparison of the graphs the dif-

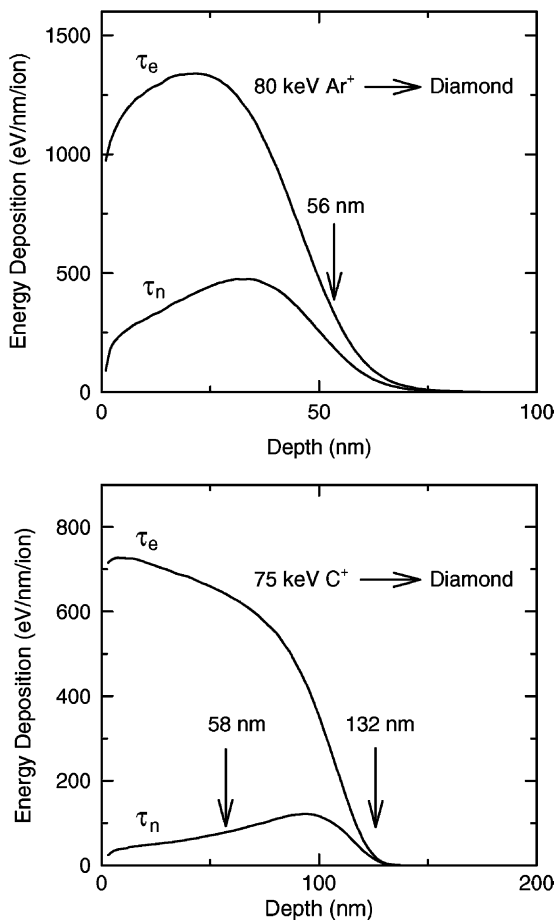


Fig. 4. Energy deposition densities per ion for elastic ( $\tau_n$ ) and inelastic ( $\tau_e$ ) collision processes as obtained from the TRIM-98 code [10]. The arrows indicate the boundaries of the amorphized layers obtained for the 80 keV argon and 75 keV carbon implantations.

ferent carbon and argon fluences must also be taken into account. For the carbon implant the boundaries of the buried graphitic layer occur at positions where energy deposition densities according to TRIM differ by more than an order of magnitude. The boundary near the surface corresponds to a graphitization energy of 27.3 eV/atom, while a value of only 0.8 eV/atom is found for the deeper interface, which agrees quite well with the results of [5]. If radiation damage would be mainly a result of elastic atomic collisions one should expect that the inner and outer interfaces occur at depths corresponding to similar graphitization energies. At this stage it is worth mentioning that the low value obtained from the boundary to the bulk is of the order expected from thermal graphitization experiments.

A similar analysis of the argon implant results in yet another graphitization energy of 11.9 eV/atom at a depth of 56 nm. In this case graphitization occurs from this interface right up to the surface. This is quite plausible, as the transferred elastic energy density per ion rises steeply above 300 eV/nm within a few nm from the surface. Surface effects can therefore play a decisive role, preventing the possible restructuring of an extremely thin diamond layer at the surface. Furthermore, the negative result obtained from the 200 keV argon implant [11] must be considered, where deposition of a damage energy density of about 15 eV/atom at the stopping power maximum is obviously not enough to destroy the dominantly  $sp^3$  character of the lattice.

From the above results it is quite clear that the condition for graphitization is not directly correlated to the damage energy density, but that other factors also play an important role. In view of the low mobility of point defects at room temperature it is unlikely that surface effects are causing the strong reduction of graphitization energy at larger depths. Taking into account the low dose rates used for the implants together with the high thermal conductivity of diamond, it is improbable that the first annealing stage at about 330 K is reached during the implantations. Furthermore, an even stronger argument against this explanation is obtained from our experimental results, which yield graphitization energies for carbon and argon

implantations differing by a factor of almost three at practically the same distance from the surface.

A previous study [11] indicated that inelastic energy deposition might be responsible for the different graphitization behaviour observed in diamond after irradiation with different ions. A comparison of the elastic and inelastic energy densities at the boundary positions immediately reveals a direct correlation between the latter two quantities, suggesting an annealing effect due to inelastic stopping. This would imply that the heated electron gas, which is formed momentarily along the tracks of the ions and their recoils, causes a reduction of damage efficiency of the elastic collision processes by defect annealing due to electron-phonon coupling. Such an effect would not depend on the accumulated energy transferred to the lattice by electronic stopping, but would rather be a function of the transferred energy density along the track of each individual ion. The graphitization energies obtained from our channeling data are therefore plotted in Fig. 5 as a function of the inelastic energy deposition densities. Despite of relatively large experimental uncertainties due to energy straggling, the graph shows convincing evidence that electronic stopping is indeed strongly increas-

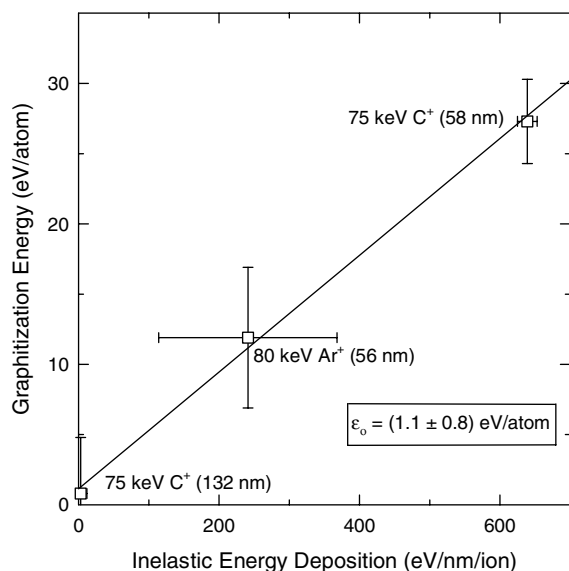


Fig. 5. Dependence of graphitization energy of diamond on the inelastic energy deposition density per ion as obtained from the TRIM-98 code [10].

ing the graphitization energy, i.e. decreasing the damage efficiency. The error flags were computed using experimental data of  $\alpha$ -particle straggling in carbon [14] and correspond to depth resolutions (FWHM) ranging from 4.0 to 6.2 nm at depths of 56 to 132 nm. The intercept with the ordinate at  $\epsilon_0 = (1.1 \pm 0.8)$  eV/atom is the graphitization energy without electronic annealing and should represent the barrier height between the ground states of the graphite and diamond phases. Although the uncertainty is quite large, its range is compatible with the thermal stability limit of diamond near the Debye temperature. Finally, the fact that the 200 keV argon implant [11] did not lead to graphitization can also be understood. The maximum damage energy density of 15 eV/atom is transferred at a depth of 87 nm, where the inelastic energy density per ion for this particular implantation is 1289 eV/nm. Comparing this with Fig. 5, it is quite obvious that conditions for graphitization are not met. For this damage energy density the formation of a graphitic layer is only expected if the accompanying inelastic energy density per ion is less than approximately 400 eV/nm.

## Acknowledgements

The authors would like to thank the Jena group of Werner Wesch for some of the implantations and Linda Prinsloo from the Chemistry Department of the University of Pretoria for the Raman analysis. Valuable discussions with Johan Prins are gratefully acknowledged.

## References

- [1] T. Evans, in: J.E. Field (Ed.), *The Properties of Diamond*, Academic Press, London, 1979, p. 403.
- [2] E. Friedland, T. Hauser, Ch. Klatt, C.M. Demanet, *Appl. Phys. A* 72 (2001) 664.
- [3] G. Braunstein, R. Kalish, *J. Appl. Phys.* 54 (1983) 2106.
- [4] N.R. Parikh, E. McGucken, M.L. Swanson, J.D. Hunn, C.W. White, R. Zuhr, in: *Proc. Int. Conf. Advanced Materials*, Tokyo, 1993.
- [5] E. Friedland, J.P.F. Sellschop, *Nucl. Instr. and Meth. B* 191 (2002) 17.
- [6] J.F. Ziegler *The Stopping and Ranges of Ions in Matter*, Vol. 4, Pergamon Press, New York, 1977.

- [7] Th. Enders, M. Rilli, H.D. Carstanjen, *Nucl. Instr. and Meth. B* 64 (1992) 817.
- [8] J.B. Marion, F.C. Young, *Nuclear Reaction Analysis*, North-Holland Publishing Company, Amsterdam, 1968.
- [9] L.C. Prinsloo, *Appl. Phys. A* 72 (2001) 658.
- [10] J.F. Ziegler, J.P. Biersack, U. Littmark, in: J.F. Ziegler (Ed.), *The Stopping and Ranges of Ions in Matter*, Vol. 1, Pergamon Press, New York, 1985.
- [11] E. Friedland, L.C. Prinsloo, *Surf. Coat. Technol.* 158–159 (2002) 64.
- [12] J.C. Bourgoin, B. Massarani, *Phys. Rev. B* 14 (1976) 3690.
- [13] J.F. Prins, T.E. Derry, J.P.F. Sellschop, *Phys. Rev. B* 34 (1986) 8870.
- [14] G. Konac, S. Kalbitzer, Ch. Klatt, D. Niemann, R. Stoll, *Nucl. Instr. and Meth. B* 136–138 (1998) 159.